# Surface engineering of the quality factor of metal coated microcantilevers

Ergincan, O.; Kooi, B. J.; Palasantzas, G.

*Published in:*
Journal of Applied Physics

*DOI:*
10.1063/1.4904191



*Publication date:*
2014

# Surface engineering of the quality factor of metal coated microcantilevers

O. Ergincan, B. J. Kooi, and G. Palasantzas

Citation: Journal of Applied Physics **116**, 224303 (2014); doi: 10.1063/1.4904191
View online: https://doi.org/10.1063/1.4904191
View Table of Contents: http://aip.scitation.org/toc/jap/116/22
Published by the American Institute of Physics

JOURNAL OF APPLIED PHYSICS **116**, 224303 (2014)

# Surface engineering of the quality factor of metal coated microcantilevers

O. Ergincan, B. J. Kooi, and G. Palasantzas[a)]
*Zernike Institute for Advanced Materials, University of Groningen, 9747 AG Groningen, The Netherlands*

(Received 16 October 2014; accepted 3 December 2014; published online 12 December 2014)

We performed noise measurements to obtain the quality factor (Q) and frequency shift of gold coated microcantilevers before and after surface modification using focused ion beam. As a result of our studies, it is demonstrated that surface engineering offers a promising method to control and increase the Q factor up to 50% for operation in vacuum. Surface modification could also lead to deviations from the known $Q \sim P^{-1}$ behavior at low vacuum pressures P within the molecular regime. Finally, at higher pressures within the continuum regime, where Q is less sensitive to surface changes, a power scaling $Q \sim P^{c}$ with $c \approx 0.3$ was found instead of $c = 0.5$. The latter is explained via a semi-empirical formulation to account for continuum dissipation mechanisms at significant Reynolds numbers $Re \sim 1$. © *2014 AIP Publishing LLC*.
[http://dx.doi.org/10.1063/1.4904191]

## I. INTRODUCTION

Gold coated silicon cantilevers with microscale and, more recently, nanoscale dimensions enable important applications in scanning probe microscopy and force spectroscopy. Relentless efforts are underway to shed light on the limits of submicron range resonators.[1–4] Hence, our understanding is broadened not only about the nature of the resonating medium but also of new pathways to obtain more accurate and wider range of information from electromechanical systems.[5,6] The need for higher composition resolution (minimum detectable mass) and sensitivity (maximum frequency shift for a given mass change) down to the molecular level is a dominant driving force strongly pushing towards nanoelectromechanical systems. The general approach for higher sensitivity is to reduce the inertial mass of the resonator. This results in extremely high frequencies up to microwaves,[7] while preserving high mechanical response with high quality (Q) factors, $Q \sim 10^3$–$10^5$,[1,7] active masses of picograms ($\sim 10^{-12}$ g),[8] ultralow heat capacities ($\sim 10^{-18}$ cal),[9] etc., Different sensor geometries and materials were also used in mass sensing technologies.[10,11]

Despite enormous progress so far, a central theme of fundamental and applied research in micro/nano-resonators is the achievement of high Q-factor, which is associated with energy dissipation. It is defined as the ratio of the stored energy $E_{stor}$ to the dissipated energy $E_{dis}$ (within an oscillation cycle) as $Q = 2\pi(E_{stor}/E_{dis})$. The larger the value of Q-factor, the higher the sensitivity of the resonance system is to external perturbations. The Q-factor determines also the level of fluctuations that degrades the spectral purity of a resonance (linewidth broadening) and determines the minimum intrinsic power with which the device can operate.[7] The total Q-factor of a resonator can be approximated by the relation $Q^{-1} = \sum_j Q_j^{-1}$ where the index j denotes intrinsic and extrinsic energy loss mechanisms.[12]

There are several theoretical and experimental studies that investigated the fundamentals of energy dissipation of microdevices.[13–16] According to the degree of surrounding gas rarefaction, three main gas pressure regimes (P) are identified: molecular regime, transition regime, and continuum regime.[17] The rarefaction regimes for high frequency oscillatory flow of MEMS can be better characterized using the Weissenberg number $Wi \equiv \omega\tau$. $\omega$ is the radial frequency, $\tau = \mu/P$ ($\tau \approx 246\,\mu$sPa/P) is the relaxation time of the surrounding fluid, $\mu$ the dynamic viscosity, and the P is the pressure.[18–20] When the $\omega\tau \ll 1$ the Newtonian approach of the Navier-Stokes approximation is valid in the continuum regime. Earlier studies elucidated the hydrodynamic loading by a frequency response model of a cantilever beam immersed in viscous fluid.[21] In the continuum regime, the interactions between the oscillating surface and the fluid molecules are characterized by the penetration depth $\lambda = \sqrt{2\mu/\omega\rho_{fl}}$ (with $\rho_{fl}$ of the surrounding fluid).[13,18,20] The transition regime, which is defined as the deviation of flow from the Newtonian, is well approximated with the $\omega\tau \approx 1$. When $\omega\tau > 1$ the Newtonian approximation is no longer valid. When the mean free path $L_{mph} = 0.23K_BT/Pd^2$, for a dilute gas of pressure P assuming the molecules as hard spheres of diameter d ($\approx 3.6\times10^{-10}$ m), is much larger than the resonator beam width w ($w < 0.1L$ with L the resonator length), and $\omega\tau \to \infty$ the intermolecular collisions are effective and this is the molecular regime.[18–20]

However, so far, experimental studies of the energy dissipation and the frequency response of metal coated microresonators with systematic surface modifications have remained unexplored. Hence, we study here the influence of surface modification of gold coated (350 nm thick) microcantilevers, which are widely used in scanning probe technology. For this purpose, different length microcantilevers but with similar widths ($\approx 30\,\mu$m) and thicknesses ($\approx 2\,\mu$m) (see for details Tables I and II) were modified by focused ion beam (FIB) along different etching directions as it is shown in Fig. 1. The patterns of the surface modifications were carefully chosen so that their influence on the Q-factor and

a)Author to whom correspondence should be addressed. Electronic mail: G.Palasantzas@rug.nl.

 

TABLE I. Properties of non-modified and modified microcantilevers.

| Type[a] | L ($\mu$m) | $f_{air}$ (kHz) | $M_{eff}$ (ng) | $k_{eff}$ (N/m) | $Q_{int}$ | $Q_{surf}$ | $\delta E_{sl}$ (MPa · m) |
|---|---|---|---|---|---|---|---|
| **A-1** | 135.6 | 152.256 | 6.30 | 5.8 | 5526 | 5554 | 10.4 |
| **A(m)-1** | | 153.257 | 5.68 | 5.3 | 5935 | 5968 | 9.6 |
| **A-2** | 127.6 | 134.528 | 6.96 | 5.0 | 3453 | 3463 | 16.6 |
| **A(m)-2** | | 135.440 | 6.31 | 4.6 | 4066 | 4080 | 14.1 |
| **A-3** | 136 | 130.499 | 5.32 | 3.6 | 3457 | 3466 | 16.6 |
| **A(m)-3** | | 132.974 | 4.70 | 3.3 | 4535 | 4551 | 12.6 |
| **B-1** | 95.1 | 326.214 | 5.09 | 21.5 | 5003 | 5053 | 11.4 |
| **B(m)-1** | | 328.150 | 4.96 | 21.2 | 5152 | 5205 | 11.1 |
| **B-2** | 87.3 | 269.203 | 3.96 | 11.4 | 4006 | 4032 | 14.3 |
| **B(m)-2** | | 271.570 | 4.07 | 11.9 | 3552 | 3573 | 16.1 |
| **B-3** | 95.6 | 272.049 | 3.98 | 11.7 | 3499 | 3519 | 16.4 |
| **B-3(m)** | | 278.708 | 3.73 | 11.5 | 4948 | 4989 | 11.5 |

[a](m) denotes modified cantilever.

resonance frequency $f_o$ vs. pressure P could be clearly observed.

## II. THEORY MODELS FOR THE QUALITY FACTOR

In high vacuum (e.g., P < 10 Pa), where the characteristic length w is much greater than the molecular mean free path, $L_{mph} \gg w\,(\omega\tau \gg 1)$, the energy losses are intrinsic and the Q (= $Q_{int}$) factor is given by

$$Q_{int}^{-1} = Q_{TED}^{-1} + Q_{clamp}^{-1} + Q_{Surface}^{-1}, \quad (1)$$

where $Q_{TED}$, $Q_{clamp}$, and $Q_{Surface}$ denote the quality factors due to thermoelastic damping, clamping, and surface losses, respectively.[3,4,22,23] The quality factors $Q_{TED}$ and $Q_{clamp}$ are not strongly influenced by surface modifications of small thickness $t_{mod} \ll t$ with t the thickness of the cantilever. The condition $t_{mod} \ll t$ is satisfied since in our case, as Fig. 1 shows, $t_{mod} \sim 60$ nm, while (see Table II) the thickness of the cantilevers is $t \sim 2\,\mu$m yielding thus $t_{mod}/t \sim 0.03$ ($\ll 1$). Energy losses due to clamping occur because of the strain at the connection area with the support base. For cantilevers with semi-infinite base or the wavelength of the shear wave in the beam is much less than the base thickness $t_b$ ($\approx 300\,\mu$m in our case), the Q-factor is given by[23]

TABLE II. Properties of non-modified and modified microcantilevers.

| Type[a] | w ($\mu$m) | t ($\mu$m) | $f_{vacuum}$ (kHz) | C[b] | $k_{eff}$[c] (N/m) | $\Delta m/m$ (%) |
|---|---|---|---|---|---|---|
| **A-1** | 30.9 | 2.2 | 152.694 | 0.33 | 5.8 | — |
| **A(m)-1** | | | 153.707 | 0.34 | 5.9 | 1.33 |
| **A-2** | 31 | 2.0 | 134.943 | 0.30 | 4.0 | — |
| **A(m)-2** | | | 135.848 | 0.33 | 4.0 | 1.34 |
| **A-3** | 31.4 | 2.0 | 130.924 | 0.35 | 4.0 | — |
| **A(m)-3** | | | 132.407 | 0.33 | 4.2 | 3.79 |
| **B-1** | 30.7 | 2.2 | 326.956 | 0.35 | 18.6 | — |
| **B(m)-1** | | | 328.945 | 0.34 | 18.8 | 1.21 |
| **B-2** | 31.4 | 1.8 | 270.040 | 0.33 | 10.1 | — |
| **B(m)-2** | | | 272.281 | 0.34 | 10.2 | 1.66 |
| **B-3** | 31 | 2.0 | 272.753 | 0.35 | 12.1 | — |
| **B(m)-3** | | | 278.482 | 0.34 | 12.7 | 4.93 |

[a](m) denotes modified cantilever.
[b]The scaling exponent "c" in the continuum regime.

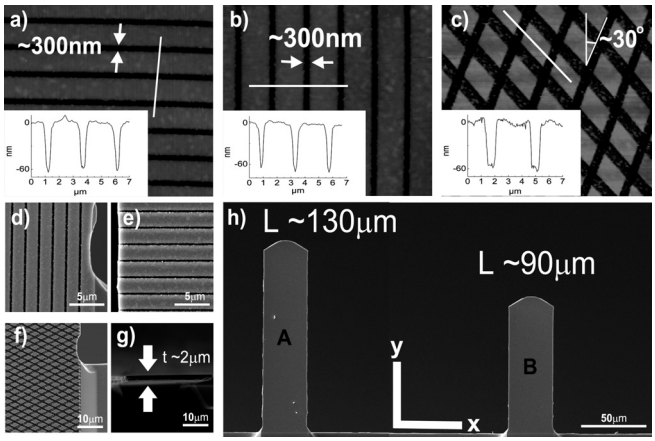


FIG. 1. Types of gold cantilever surface modification. (a) AFM image of type-(1) gold surface modification, RMS (~30 nm), $\rho_{rms} \sim 0.7361$; (b) AFM image of type-(2) gold surface modification, RMS ~ 21.4 nm, $\rho_{rms} \sim 0.721$; (c) AFM image of type-(3) gold surface modification, RMS ~ 26.5 nm, $\rho_{rms} \sim 0.589$; SEM image of A with surface modification (d) type-(1); (e) type-(2); (f) type-(3); (h) SEM image of gold coated cantilevers of different lengths before surface modification (~130 and ~90 $\mu$m) denoted as A and B, respectively, similar widths (~30 $\mu$m.), and (g) thickness's (~2 $\mu$m). Insets of (a)–(c) show the height profile of the modified surfaces.

$$Q_{clamp} = 0.95\,\frac{1}{w}\frac{t_b^2}{t^2}. \quad (2)$$

Moreover, the $Q_{TED}$ due to thermoelastic dissipation (associated with thermal currents generated by vibratory volume changes in elastic media with non-zero thermal-expansion coefficient) is given by[24]

$$\frac{1}{Q_{TED}} = \frac{E\alpha_T^2 T}{C_p \rho}\left(\frac{6}{\zeta^2} - \frac{6}{\zeta^3}\frac{\sinh\zeta + \sin\zeta}{\cosh\zeta + \cos\zeta}\right). \quad (3)$$

E is the Young's modulus, $\alpha_T$ is the thermal expansion coefficient, $C_p$ is the specific heat at constant pressure, T is the system temperature, $\rho$ is the material density of the cantilever, and $\zeta = t\sqrt{(\omega\rho C_P)/2\kappa}$ where $\kappa$ the thermal conductivity of the cantilever.[24] Finally, we consider the surface losses to originate from a thin surface layer of complex modulus $E_{sl}$ due to the disruption of the atomic lattice by a thin layer of surface contamination.[4,24] Although this layer does not influence drastically the energy stored in the cantilever, it can enhance energy dissipation and $Q_{Surface}$ is given by[4]

$$Q_{Surface} = \frac{2(3w + t)}{wt}\frac{\delta E_{sl}}{E} \quad (4)$$

with $\delta$ the thickness of the surface layer and $E_{sl} = \mathrm{Im}[E_s]$.[4,24]

For extrinsic dissipation in medium-vacuum (e.g., $10^1\mathrm{Pa} < P < 10^3\mathrm{Pa}$), we are within the molecular regime where $L_{mph} > w$ (or $\omega\tau > 1$). The quality factor is given by[7,18,19]

$$Q_{Mol} = \left[\frac{M_{eff}\omega_o v}{P}\right]\frac{1}{S_{Total,1}}. \quad (5)$$

$M_{eff}$ is the effective resonating mass of the cantilever, and $\omega_o$ is the angular resonance frequency in vacuum. $S_{total,1}$ is the corresponding surface area of the resonator, and

$\upsilon = \sqrt{k_B T/m_r}$ is the thermal velocity of impinging molecules of mass $m_r$ at absolute temperature T. In the molecular regime the quality factor scales with gas pressure P as $Q \propto 1/P$,[7,18,19] while it changes to $Q \propto 1/P^{0.5}$ in the continuum regime (see, e.g., Fig. 2).[25]

With further increment of the pressure the surrounding gas acts as a viscous fluid ($\omega\tau \leq 1$). The microcantilevers, having a plate-like shape immersed in fluid can be dominated by dissipation due to: acoustic radiation, squeeze-film, and viscous losses. Squeeze film loss can be significant when there is a narrow gap between a vibrating and a stationary element,[26,27] which is not relevant in our case. In any case, the quality factor due to dominant viscous losses is given by[28–30]

$$Q_{Fluid} = \frac{k_d}{\rho w \omega_R^2 S_{Total,2} \Lambda(Re)}. \quad (6)$$

$\Lambda(Re) = aRe^{-0.7}$ is a dimensionless hydrodynamic function (a is a constant coefficient specific for each type of cantilever), $Re = (\rho w^2 \omega_0)/4\mu$ is the Reynolds number, $k_d$ is the dynamic spring constant, and $\rho = PM_m/RT$ is the density of the ideal gas with R the gas constant and $M_m$ the gas molar mass, and $\omega_R$ is the resonance frequency at the measured pressure.[30] $S_{Total,2}$ is the surface area of the cantilever associated with the $Q_{Fluid}$ in the dense regime.

## III. EXPERIMENTAL PROCEDURE

Noise measurements were performed (see supplementary material for a typical noise spectrum in Fig. 1S)[31–34] to determine the Q-factor as a function of vacuum pressure P for as received and surface modified cantilevers as it is shown in Figs. 1, 2, and 4. The experiments were conducted for cantilevers with two different lengths, denoted as A and B (Fig. 1(h)). They were modified using FIB in various etching directions: x and y are the coordinate notations of the cantilever's surface plane (Fig. 1(h)). Etching in the y-direction (along the length of the cantilever, Fig. 1(d)) is denoted as (1), etching in the x-direction (along the width of the cantilever, Fig. 1(e)) is denoted as (2), and etching at $\pm 30$ angles with respect to the y-direction, Fig. 1(f)), is denoted as (3). All grooves are $\cong 2\,\mu$m apart from each other, while the etching depth is $\cong 60$ nm (insets of Figs. 1(a)–1(c)). In addition, the dimensions of each cantilever were confirmed using a scanning electron microscope (SEM: Figs. 1(d)–1(f)). This is important for the comparison of the effective surface area $S_{Total,i(=1,2)}$, obtained from the fittings of the Q vs. P data in different pressure regimes (corresponding to different dissipating mechanisms) with the geometric value $S_{Total}$. The latter is obtained using AFM morphology data as input into the expression[35]

$$\frac{S_{Total}}{S_{smooth}} = \int_0^{+\infty} du \sqrt{1 + \rho_{rms}^2 u e^{-u}}, \quad (7)$$

with $\rho_{rms}$ the average local surface slope.

## IV. RESULTS AND DISCUSSION

From the Q vs. P plots in Fig. 2, the free molecular (saturated) regime yields $Q_{int}$ allowing thus calculation of $Q_{Surface}$ (after subtraction of $Q_{TED}$ and $Q_{clamp}$ obtained via Eqs. (2) and (3)) via Eq. (4). Indeed, calculations of Q vs. P are shown in Fig. 2 for different values of $\delta E_{sl}$.Subsequently, using the value of $\delta E_{sl}$ that matches the Q-factor data, the product $\delta E_{sl}$ is estimated via Eq. (4) to have an average value $\delta E_{sl} \approx 14$MPa · m for the unmodified cantilevers (cantilevers A and B in Table I). The latter implies that $E_{sl}$ is significantly smaller than the Young modulus E (~130–180 GPa for Si) of the resonating medium. Moreover, multi-directional surface modification for this regime allows the investigation of

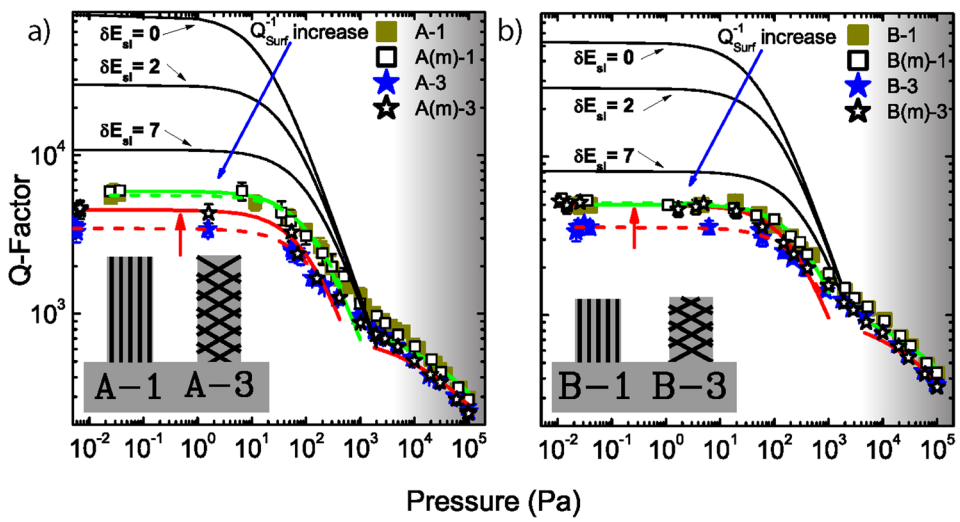


FIG. 2. Q-factor vs. pressure P for cantilever types A and B with dimensions given in Figs. 1(a) and 1(b) The corresponding surface modifications (1, 3) are illustrated in the insets (a) and (b). The index "m" denotes the modified cantilevers as shown in Fig. 1. (a) and (b) The fits shown by the red and the green dashed lines in the molecular regime illustrate the $Q \sim 1/P$ scaling of Eq. (5), respectively, for A and B unmodified cantilevers. The solid black lines are the calculated $Q^{-1}$ $(=Q_{int}^{-1} + Q_{Mol}^{-1})$ with $\delta E_{sl} = 0$, 2, and 7. The increase in the surface related energy dissipation is shown with the blue arrows. (a) and (b) The fits shown by the red and the green solid lines in the molecular regime illustrate the $Q \sim 1/P$ scaling of Eq. (5), respectively, for A and B modified cantilevers. The small red arrows depict the increase in the $Q_{int}$ after the surface modification. (a) and (b) Fits in the continuum regime (illustrated with the gradient gray background): red and green fit lines depicts the $Q \sim 1/P^{0.5}$ scaling.

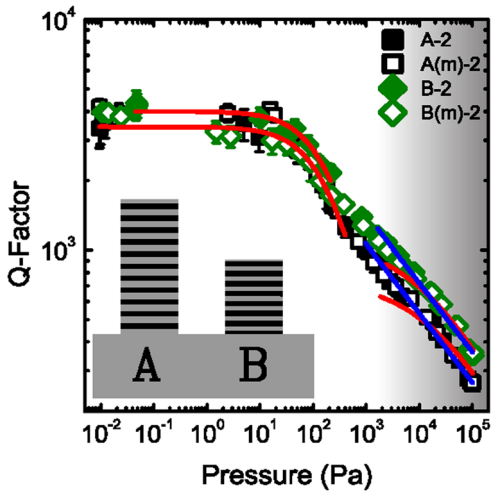


FIG. 3. Q-factor vs. pressure P for cantilever types A in Fig. 1. The corresponding surface modification (2) is illustrated in the insets. The index ''m'' denotes the modified cantilevers as shown in Fig. 1. The red fitting lines illustrate the 1/P scaling behavior in the molecular regime and $Q \sim 1/P^{0.5}$ scaling behavior in the continuum regime. Blue lines illustrate the $Q \sim 1/P^{0.3}$ scaling.

the influence of anisotropic surface structures and also possible residual stress release that is built within the metal coating of the cantilevers.

Furthermore, it is important to analyze our results according to gas rarefaction. Hence, we start with some important outcomes of the intrinsic dissipation regime ($P \leq 10$ Pa) where $Q \approx Q_{int}$. The calculation of the removed mass during surface modification, both using the simple assumption of the frequency shift due to mass change $\Delta m \approx 2m(\Delta f/f)$ ($\Delta m$ is the mass removed, and m is the total mass) and the calculations by geometrical means, show that for type-(1) and type-(2) surface modifications the amount of removed mass was ≈1.5% of the total mass (see also Table II). The influence of the removed mass on the Q-factor for both cantilevers A and B with type-(1) surface modification is within the standard ∼10% measurement error as depicted in Figs. 2 and 3. We have further analyzed the mass removal influence on the Q-factor, in the intrinsic regime, by including a trapezoidal metal coated cantilever (Figs. 4 and 5). We have removed mass from the surface of the device using the FIB as it is shown in the inset of Fig. 5. The change in the frequency of the cantilever after mass removal was corresponding to ≈2% of the total mass (see Fig. 6). Nonetheless, the Q-factor vs. P graph in Fig. 5 showed the same negligible change of the $Q_{int}$ within the standard error of the measurement similar to the type-(1) and type-(2) modified cantilevers. However, for type-(3) surface modification, even though the removed mass was not larger than ≈4% of the total mass, the increase in the Q-factor is clearly observable and it is ∼50% larger for both A and B cantilevers in Fig. 2.

Although previous studies have shown that clamping losses as the dominant loss mechanism for the intrinsic regime,[32] our Q-factor measurements of samples A and B with type-(1) and type-(2) surface modifications have not shown any distinct behavior for the Q-factor due to differences of the cross section areas of the clamping part. Note that clamping losses are known to be directly correlated to the cross-section area of the clamping part.[23] Accordingly, if we assume surface losses as the only cause of energy dissipation, then the calculated values of the product $\delta E_{sl}$ (see Table I) characterizing the $Q_{Surface}$, by subtracting $Q_{clamp}$ and $Q_{TED}$ from the $Q_{int}$ and then using Eq. (4), shows the decrease in the surface energy.

One might also expect the cause for the increase of $Q_{int}$ for type-(3) surface modification to be the result of a change in the physical properties of the cantilevers due to FIB patterning leading to drastic changes of the structure of the cantilevers. For this purpose, we compared by the spring constant measurements before and after surface modification. Indeed, $k_{eff}$ is a physical property, which depends on the elastic modulus (E) and the cantilever dimensions. Calculations of both thermoelastic dissipation[12] and clamping losses[23] require knowledge of E of the resonating

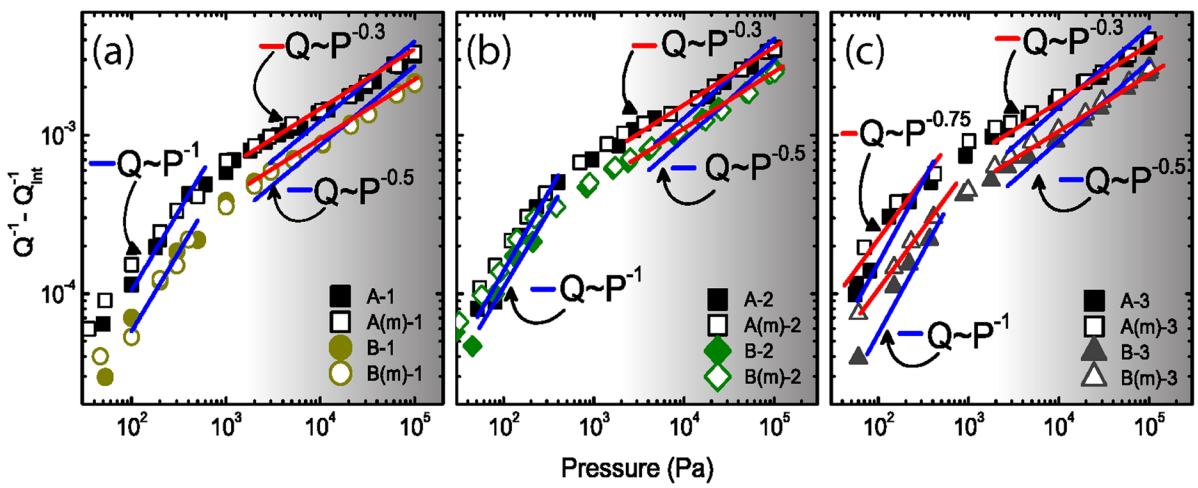


FIG. 4. Energy Dissipation vs. pressure P for cantilever types A and B with dimensions given in Figs. 1. (a)–(c) $Q^{-1}$–$Q_{int}^{-1}$ vs. P plots for cantilever types A and B with dimensions given in Fig. 1. The blue lines indicate the scaling behavior in the molecular regime with c = 1 and in the continuum regime with c = 0.5 (as indicated with arrows in Figs. (a)–(c)). The red lines to illustrate the actual $Q \sim P^{-c}$ scaling; in the molecular regime c = 0.75 (as indicated in Fig. (c) for Type-3 modification) and the continuum regime c = 0.3. (Figs. (a)–(c)).

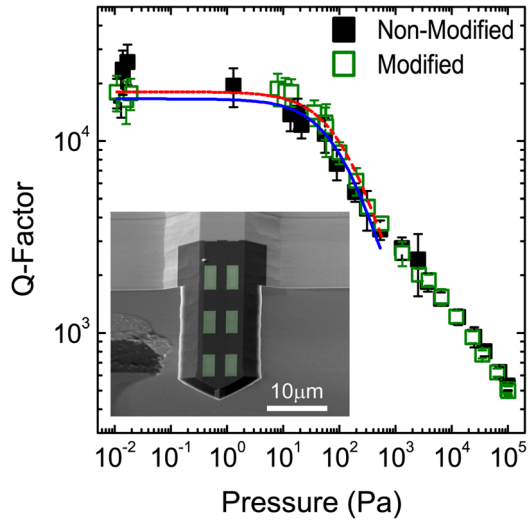


FIG. 5. Q-factor and Frequency vs. pressure P for a phase change material (PCM: $Ge_7Sb_{93}$) coated cantilever before and after surface modification. Q-factor vs. P of 50 nm PCM coated cantilever before (black squares) and after FIB milling (green squares) as depicted in the SEM image in the inset (the FIB milled part of the cantilever surface is dark colored and the remaining part is falsely colored in green). The red and the blue solid fitting lines show the negligible difference of the Q-factor in the intrinsic regime between the modified and non-modified cantilevers.

medium. For this reason besides the Q-factor, an accurate measurement of the cantilever spring constant $k_{eff}$ is essential for a meaningful calibration of the resonator as a sensor. In fact, it is possible to acquire by the Thermal tuning method the value of $k_{eff}$ and the resonance frequency $f_0(=\omega_0/2\pi)$ with an accuracy down to ~10% and ~1%, respectively.[33] In fact, as Table I indicates, there is no significant discrepancy between the $k_{eff}$ of the non-modified and modified cantilevers. Consequently, for the type-(3) surface modification, the ~50% increase of the intrinsic $Q_{int}$ factor can be related to the relaxation of surface residual stress by the creation of small micrometer size gold patches or by surface strain induced change in the curvature of the cantilever. Other possible factors, such as relaxation of defects under oscillating strain and $Ga^+$ ions induced defect states, are

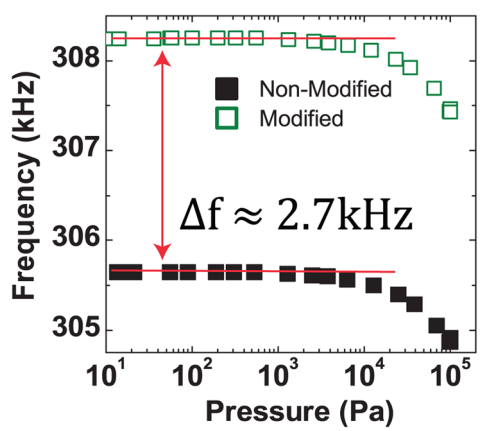


FIG. 6. Frequency vs. P of the modified and non-modified cantilevers to indicate the measured frequency shift $\Delta f \sim 2.7$ kHz due to mass removal upon modification.

expected to affect all of the modified cantilevers regardless of the directionality of the gold surface modification. Therefore, they can be excluded as possible reasons contributing to dissipation mechanisms.

In addition, one of the main reasons that also inspired the patterning of the resonator surfaces with anisotropic corrugations (grooves) in various plane directions was to observe possible differences in the scaling behavior of Q-factor vs. P for both the molecular and continuum regimes from what is known in the literature (Figs. 4(a)–4(c)). Indeed, from literature, it is expected the known scaling behavior, $Q \sim P^{-c}$ where the scaling exponent c is "−1" and "−0.5" for the molecular and the continuum regime, respectively.[19,33] The $Q \sim P^{-1}$ scaling predicted by Eq. (5) is almost confirmed for both non-modified and modified cantilevers of type-(1) and type-(2) for both samples A and B (Figs. 4(a) and 4(b)). As a matter of fact no change is observed from the known scaling characteristics of type-(1) and type-(2) surface modifications in any of the gas rarefaction regimes (see Figs. 2(a) and 4(a)). For the type-(3) surface modification some slight variation of the scaling behavior was observed for the modified cantilevers (Fig. 4(c)). The average energy dissipated by considering the shear stress on cantilever surface is evidently altered by the increased number of patch edges on the surface leading to increased energy dissipation ($Q \sim P^{-0.75}$, Fig. 4(c)).

As it can be observed in Figs. 4(a)–4(c), the transition to the continuum regime is not sensitive to surface structure modifications, and the Q-factor values of the modified cantilever converge to similar values as the non-modified cantilevers. In contrast with the molecular regime, in the continuum regime, we observed a significant deviation in the scaling behavior of the Q-factor as a function of pressure from the $P^{-0.5}$. We have demonstrated this deviation with the linear fits in Figs. 4(a)–4(c). As it is shown in Figs. 4(a)–4(c) the scaling follows the behavior with $c \approx 0.3$ for both modified and non-modified cantilever surfaces. This scaling behavior has also been reported in Refs. 19 and 30, and it can be explained as follows. The power law behavior of the dimensionless hydrodynamic function ($\Lambda(Re)$) in Eq. (6) was explained by Sader *et al.*[30] by considering the asymptotic limits of the Reynolds number (Re): For $Re \ll 1$ the hydrodynamic function scales as $\Lambda(Re) \sim Re^{-1}$, while for $Re \gg 1$ it scales as $\Lambda(Re) \sim Re^{-0.5}$.[30] Thus, an intermediate power-law dependence during the measurement is possible since for our system we have significant Reynolds numbers ($Re \sim 1$). Moreover, for ideal surrounding gas, we obtain the scaling behavior $\Lambda(Re) \sim Re^{-0.7}$,[30] which after substitution into Eq. (6) yields

$$Q_{Fluid} = \left[ k_d \omega_R^{-1.3} \left( \frac{w^2}{4\mu} \right)^{0.7} a^{-1} \left( \frac{M_m}{RT} \right)^{-0.3} \right] \frac{P^{-0.3}}{S_{Total,2}}. \quad (8)$$

From Eq. (8), it is evident the scaling behavior $Q \sim P^{-0.3}$ observed experimentally during our measurements. Moreover, it is also possible to calculate Q-factor for any cantilever with similar plane surfaces by simple spring constant measurement[33] with the assumption of hydrodynamic

TABLE III. Surface area values of modified and non-modified microcantilevers.

| Type[a] | $S_{Total}$ ($\mu m^2$) | $S_{Total,1}$ ($\mu m^2$) | $S_{Total,2}$ ($\mu m^2$) |
|---|---|---|---|
| **A-1** | 4190 | 3550 | 4291 |
| **A(m)-1** | 4227 | 3710 | 4010 |
| **A-2** | 3956 | 3710 | 4841 |
| **A(m)-2** | 4079 | 4190 | 4432 |
| **A-3** | 4266 | 3050 | 3802 |
| **A(m)-3** | 4328 | 3170 | 3706 |
| **B-1** | 2700 | 2750 | 2876 |
| **B(m)-1** | 2724 | 2650 | 2931 |
| **B-2** | 2610 | 1930 | 2551 |
| **B(m)-2** | 2691 | 2950 | 2567 |
| **B-3** | 2852 | 1900 | 2498 |
| **B(m)-3** | 2893 | 2120 | 2434 |

[a](m) denotes modified cantilever.

loading being the dominant loss mechanism in the continuum regime and using Eq. (8).[30,34]

Finally, we have to stress that besides the enhanced hydrodynamic damping in the continuum regime, the resonators undergo also changes in their effective mass due to mass loading resulting in significant frequency shifts. The scaling $Q \sim P^{-0.5}$ was also observed in Ref. 25 and it was explained as a result of mass loading. Here, however, despite the drastic alterations of the surface structure, the change in surface area was less than 1% of the total surface area. The latter could be the reason why we did not observe a measurable difference neither in the Q-factors (Figs. 2(a) and 2(b)) nor in the frequency shifts due to viscous loading between the modified and non-modified resonators. The surface area values calculated from the fittings of Eq. (5) and (6) are comparable to the geometric area values $S_{Total}$ as it can be seen in Table III, while deviations for some values of $S_{Total,1}$ appear to occur. This can be partly understood from the fact that the effective resonating surface area can differ from the geometric one, but further investigations are still necessary to understand the precise nature of these deviations.

## V. CONCLUSIONS

We have demonstrated a different approach to quality factor engineering by patterning the metal coating of commercially available microcantilevers. Our work shows that surface engineering gives promising results, as the intrinsic quality factors could be increased even up to 50% depending surface patterning during vacuum operations. In the molecular regime, the quality factor decays with increasing pressure P as $Q \sim 1/P$, while some deviations from this scaling might take place depending on the surface modification. However, in the continuum regime, comparing modified and non-modified cantilevers, the Q-factors become less sensitive to surface modifications. In the continuum regime, a semi-empirical formulation for Q-factor with scaling $c \approx 0.3$ instead of $c = 0.5$ was given to explain also the obtained scaling exponents from the measured Q data vs. P. Finally, the obtained surface areas of the cantilevers indicate that the effective resonating surface area can differ from the geometric one, but further studies are necessary in this direction.

## ACKNOWLEDGMENTS

The authors would like to acknowledge financial support by the STW grant 10082, and G.H. ten Brink for the SEM images.

[1]K. L. Ekinci, Y. T. Yang, and M. L. Roukes, J. Appl. Phys. **95**, 2682 (2004).
[2]A. N. Cleland and M. L. Roukes, Appl. Phys. Lett. **69**, 2653 (1996).
[3]A. B. Hutchinson, P. A. Truitt, K. C. Schwab, L. Sekaric, J. M. Parpia, H. G. Craighead, and J. E. Butler, Appl. Phys. Lett. **84**, 972 (2004).
[4]K. Y. Yasumura, T. D. Stowe, E. M. Chow, T. Pfafman, T. W. Kenny, B. C. Stipe, and D. Rugar, J Microelectromech. Syst. **9**, 117 (2000).
[5]O. Sahin, S. Magonov, C. Su, C. F. Quate, and O. Solgaard, Nat. Nanotechnol. **2**, 507 (2007).
[6]R. Garcia and E. T. Herruzo, Nat. Nanotechnol. **7**, 217 (2012).
[7]K. L. Ekinci and M. L. Roukes, Rev. Sci. Instrum. **76**, 061101 (2005); S. M. Meenehan, J. D. Cohen, S. Gröblacher, J. T. Hill, A. H. Safavi-Naeini, M. Aspelmeyer, and O. Painter, Phys. Rev. A **90**, 011803(R) (2014); D. T. Nguyen, C. Baker, W. Hease, S. Sejil, P. Senellart, A. Lemaître, S. Ducci, G. Leo, and I. Favero, Appl. Phys. Lett. **103**, 241112 (2013).
[8]Y. T. Yang, C. Callegari, X. L. Feng, K. L. Ekinci, and M. L. Roukes, Nano Lett. **6**, 583 (2006).
[9]H. Ibach, Surf. Sci. Rep. **29**, 195 (1997).
[10]B. Ilic, H. G. Craighead, S. Krylov, W. Senaratne, C. Ober, and P. Neuzil, J. Appl. Phys. **95**, 3694 (2004).
[11]H. G. Craighead, Science **290**, 1532 (2000).
[12]P. Mohanty, D. A. Harrington, K. L. Ekinci, Y. T. Yang, M. J. Murphy, and M. L. Roukes, Phys. Rev. B **66**, 085416 (2002).
[13]K. Park, J. Shim, V. Solovyeva, E. Corbin, S. Banerjee, and R. Bashir, Appl. Phys. Lett. **100**, 154107 (2012).
[14]F. Sharipov and D. Kalempa, Phys. Fluids **19**, 017110 (2007).
[15]J. Linden and E. Oesterschulze, Appl. Phys. Lett. **100**, 113511 (2012).
[16]D. R. Emerson, X.-J. Gu, S. K. Stefanov, S. Yuhong, and R. W. Barber, Phys. Fluids **19**, 107105 (2007).
[17]A. Pandey, R. Pratap, and F. Chau, Exp. Mech. **48**, 91 (2008).
[18]K. L. Ekinci, D. M. Karabacak, and V. Yakhot, Phys. Rev. Lett. **101**, 264501 (2008).
[19]D. M. Karabacak, V. Yakhot, and K. L. Ekinci, Phys. Rev. Lett. **98**, 254505 (2007).
[20]K. L. Ekinci, V. Yakhot, S. Rajauria, C. Colosqui, and D. M. Karabacak, Lab Chip **10**, 3013 (2010).
[21]J. E. Sader, J. Appl. Phys. **84**, 64 (1998).
[22]S. Evoy, A. Olkhovets, L. Sekaric, J. M. Parpia, H. G. Craighead, and D. W. Carr, Appl. Phys. Lett. **77**, 2397 (2000).
[23]J. A. Judge, D. M. Photiadis, J. F. Vignola, B. H. Houston, and J. Jarzynski, J. Appl. Phys. **101**, 013521 (2007).
[24]R. Lifshitz and M. L. Roukes, Phys. Rev. B **61**, 5600 (2000).
[25]O. Svitelskiy, V. Sauer, N. Liu, K.-M. Cheng, E. Finley, M. R. Freeman, and W. K. Hiebert, Phys. Rev. Lett. **103**, 244501 (2009).
[26]S. T. Hansen, A. Turo, F. L. Degertekin, and B. T. Khuri-Yakub, in *2000 IEEE Ultrason. Symp.* (2000), Vol. 1, pp. 947–950.
[27]C. Lissandrello, V. Yakhot, and K. L. Ekinci, Phys. Rev. Lett. **108**, 084501 (2012).
[28]J. E. Sader, J. W. M. Chon, and P. Mulvaney, Rev. Sci. Instrum. **70**, 3967 (1999).
[29]C. A. Van Eysden and J. E. Sader, J. Appl. Phys. **100**, 114916 (2006).
[30]J. E. Sader, J. A. Sanelli, B. D. Adamson, J. P. Monty, X. Wei, S. A. Crawford, J. R. Friend, I. Marusic, P. Mulvaney, and E. J. Bieske, Rev. Sci. Instrum. **83**, 103705 (2012).
[31]See supplementary material at http://dx.doi.org/10.1063/1.4904191 for a Cantilever Noise spectrum and its Lorentzian fit.
[32]O. Ergincan, G. Palasantzas, and B. J. Kooi, Phys. Rev. B **85**, 205420 (2012).
[33]B. Ohler, Rev. Sci. Instrum. **78**, 063701 (2007).
[34]O. Ergincan, G. Palasantzas, and B. J. Kooi, Rev. Sci. Instrum. **85**, 026118 (2014).
[35]B. N. J. Persson, J. Chem. Phys. **115**, 3840 (2001); G. Palasantzas, Phys. Rev. B **48**, 14472 (1993).